JOURNAL OF Materials CHEMISTRY

Synthesis and photoluminescence of single-crystalline In_2O_3 nanowires

X. S. Peng,* G. W. Meng, J. Zhang, X. F. Wang, Y. W. Wang, C. Z. Wang and L. D. Zhang

Institute of Solid State Physics, Chinese Academy of Sciences, Hefei 230031, P. R. China. E-mail: zyzhao@mail.issp.ac.cn; Fax: +86-0551-5591434

Received 12th December 2001, Accepted 5th March 2002
First published as an Advance Article on the web 3rd April 2002

Single-crystalline In_2O_3 nanowires have been successfully synthesized from indium grains by a vapor–solid method at 1030 °C in 90% Ar and 10% O_2 atmosphere. These nanowires are uniform with diameters of 40–120 nm and lengths of about 15–25 μm, and crystallize in a cubic structure. The growth of these nanowires is controlled by a spiral growth mechanism. Photoluminescence (PL) measurements show a green–blue PL band in the wavelength range of 400–700 nm with a peak at 470 nm (2.64 eV), caused by oxygen vacancies in the In_2O_3 nanowires.

Introduction

Recent progress in the synthesis of nanowires has been driven by the need to understand the novel physical properties of one-dimensional nanoscale materials, and their potential application in constructing nanoscale electronic and optoelectronic devices.[1] Up to now, much attention has been paid to the preparation of nanowires of the family of oxides with interesting optical and electrical properties. Several binary oxide nanowires such as GeO_2,[2] Ga_2O_3,[3] MgO[4] and SiO_2[5] have been successfully synthesized. Very recently, ZnO, CdO, SnO_2 and In_2O_3 nanobelts have also been fabricated by the thermal evaporation method.[6] Among them, In_2O_3, a wide band gap transparent conductor (with a direct band gap of about 3.6 eV and an indirect band gap of about 2.6 eV), has been widely used in the electronic field as window heater, solar cell, and flat-panel display materials.[7,8] Previous studies mainly focused on the indium oxide films or nanoparticles.[9,10] In contrast, the investigation on wire-like In_2O_3 nanostructures is quite limited. Recently In_2O_3 nanofibers have been synthesized by the catalytic growth from InP,[11] and polycrystalline In_2O_3 nanowires by electrodepositing metallic indium into the channels of anodic alumina membranes and subsequent oxidization.[12] Although photoluminescence (PL) has already been observed in some In_2O_3 films and nanostructures,[9–12] the PL mechanism is still not clear. Here, we report an efficient route for the synthesis of In_2O_3 nanowires in high yield entailing a rapid heating process from indium grains at 1030 °C in a mixture of Ar and O_2, and we have studied the PL properties of the In_2O_3 nanowires at room temperature.

Experimental details

The preparation of the cubic In_2O_3 nanowires is briefly described as follows. The indium grains (99.999% purity) with diameters of 1–3 mm loaded in a ceramic boat were put into the center of a horizontal quartz tube with diameter of 3 cm and length of 60 cm. The quartz tube was placed in a conventional tubular furnace. Before heating, the quartz tube was filled with a mixture of gas comprising 90% argon and 10% oxygen with a flow rate of 100 cm^3 min^{-1}. The temperature of the furnace was increased at a fast rate to 1030 °C from room temperature in 5 min and kept at this temperature for 2 hours. After the system had cooled down to room temperature, light-yellow wool-like products on the ceramic boat wall were found. The products were characterized by X-ray powder diffraction (XRD) (PW 1710 instrument with Cu-Kα radiation), scanning electron microscopy (SEM) (JEOL JSM-6300) and transmission electron microscopy (TEM) (JEM 200CX) and high resolution transmission electron microscopy (HRTEM) (JEOL 2010, operated at 200 kV), energy-dispersive X-ray fluorescence (EDX) (EDAX, DX-4) attached to the JEOL 2010. For SEM observations, the product was pasted on the Al substrate by carbon conducting paste. For TEM observation, the as-synthesized products were ultrasonically dispersed in ethanol and a drop was then placed on a copper grid coated with amorphous carbon. PL spectra were obtained using a Hitachi 850-fluorescence spectrophotometer with Xe lamp at room temperature. For PL observation, the products were collected from the wall of the ceramic boat. The electron paramagnetic resonance (EPR) spectrum was carried out by using a Bruker ER-200D electron paramagnetic resonance device with 10 dB (20 mW).

Results and discussion

Morphology and structure of the synthesized In_2O_3 nanowires

Fig. 1 shows a typical XRD pattern of the products. The diffraction peaks can be indexed to In_2O_3 with a cubic structure of the bixbyite Mn_2O_3 (I) type (also called the C-type rare-earth

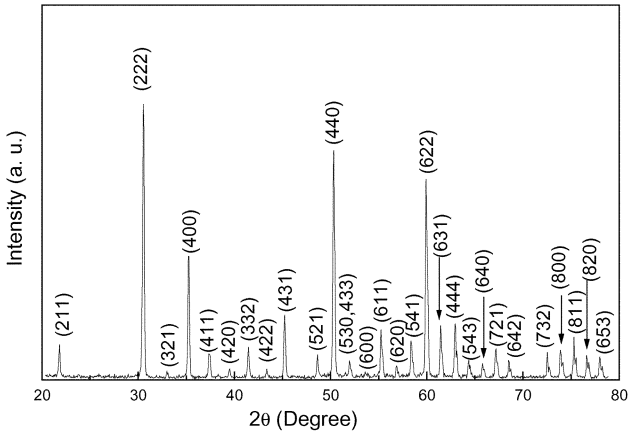

Fig. 1 The XRD pattern of the as-synthesized In_2O_3 nanowires.

 DOI: 10.1039/b111315a

oxide structure)[13] with cell constant of $a = 1.012$ nm. No unreacted elemental indium was detected. A typical SEM image of the products (Fig. 2) shows that uniform In_2O_3 nanowires were formed in a high yield. The diameters of the nanowires range from 40 to 120 nm and their lengths are 15–25 μm. Fig. 3 (a) shows a typical TEM image of two In_2O_3 nanowires, one with a cone-tip end and the other thinner wire with a diameter of about 40 nm. Actually, a conical tip at the end of every nanowire was observed in this study (see Fig. 3 (b)). Selected area electron diffraction (SAED) pattern (insert in Fig. 3 (a)) reveals that these In_2O_3 nanowires are single crystals, the surfaces enclosed by the {001} plane are similar to those of In_2O_3 nanobelts.[6] Furthermore, the HRTEM is employed to observe the fine structure of the nanowire. The corresponding HRTEM image, Fig. 3 (c), shows the fine structure of the part of the smaller wire shown in Fig. 3 (a). In this picture, the crystal lattice fringes are spaced 0.357 nm apart. This finding is in agreement with the d value of the (220) planes of the In_2O_3 crystal. The corresponding EDX result (Fig. 3 (d)) reveals that the nanowires are only composed of In and O elements (with the atomic ratio of O and In being 1.43 compared to 1.5 of the In_2O_3 phase). The Cu peaks in this spectrum are due to background from the copper TEM grid.

Growth mechanism

It is well known that two models exist to explain the growth mechanism of one-dimensional materials.[14] One is the conventional spiral growth mechanism, which concerns the existence of a screw dislocation whose line is parallel to the axis of the whisker or nanowire. In this model, the spiral plane perpendicular to the dislocation line provides a growth step, which serves as a low-energy site, so that the growth rate along the axis direction is much faster than that of the radius direction, and there exists a conical tip at one end of the nanowire or whisker.[15,16] The other is the vapor–liquid–solid (VLS) mechanism, in which an intermediate nanoparticle is located at one end of the nanowire and serves as catalyst between the vapor feed and the solid growth.

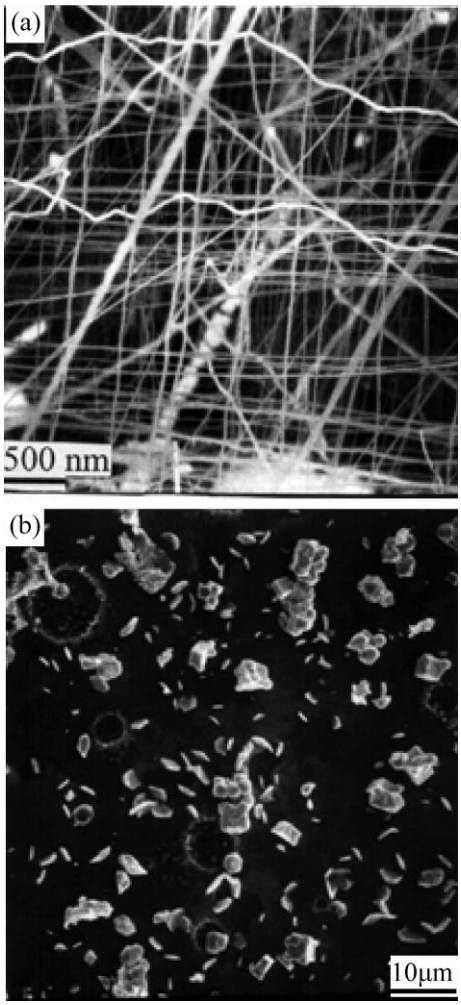

Fig. 2 (a) A typical SEM image of the as-sythesized In_2O_3 nanowires. (b) A SEM image of In_2O_3 particles prepared at 980 °C.

In this work, TEM observations reveal that there is no evidence that the In_2O_3 nanowire growth matches the VLS mechanism for two reasons. Firstly, there are no nanoparticles at the tip of any nanowire. Secondly, the source material used in our synthesis is an indium grain without any other intermediate. The conical tip at the end of every nanowire (Fig. 3 (a) and (b)) is evidence of the spiral growth mechanism.[15–18] It is likely that the growth is controlled by the spiral growth mechanism through a vapor–solid process.[19] Herein, the indium vapor evaporated from the indium particles, reacted with O_2 at the high-temperature zone (1030 °C) to form In_2O[20] and In_2O_3 (further oxide from In_2O) molecules. Then the In_2O and In_2O_3 molecules were carried by the flowing argon gas and directly deposited onto the wall of the ceramic boat at a lower temperature region (about 1000 °C), nucleating, adsorbing oxygen and growing into nanowires through the spiral growth mechanism. Since the conical tip at the end of the nanowire is highly curved, it acts as the energetically favorable site for adsorbing the molecules or clusters from the vapor, leading eventually to the one-dimensional growth of In_2O_3 nanowires.

By variation of the experiment parameters, such as lowering the temperature, absence of carrier gas and slowing the heat rate, the morphology of the products could be varied. If the temperature is lower than 1030 °C, for example, 980 °C, the products were just particles. A typical SEM image of these particles is shown in Fig. 2b. The same result also was obtained if the heating was slow (10 °C min^{-1}) or without carrier gas. All these conditions decrease the vapor of the reacting region and result in the formation of particles.

Optical properties

The PL spectrum of the In_2O_3 nanowires was measured at room temperature. It is known that bulk In_2O_3 cannot emit light at room temperature.[18] However, the present measurement (Fig. 4) shows a strong and broad PL emission spectrum from the In_2O_3 nanowires, which is mainly located in the blue–green region and peaked at 470 nm (2.64 eV) upon excitation at 382 nm (3.24 eV) at room temperature. The following PL peaks have been reported and mainly attributed to the effect of the oxygen deficiencies, *i.e.*, at 480 and 520 nm from In_2O_3 nanoparticles,[9] a peak at 637 nm from In_2O_3 films,[10] at 470 nm from In_2O_3 nanofibers,[11] and at 465 nm from In_2O_3 nanowires embedded in anodic alumina membranes.[12] The emission peak is commonly referred to as a deep-level or trap-state emission. For our In_2O_3 nanowires, the diameters seem to be too large to show a quantum confinement effect (the critical Bohr radius of In_2O_3 is about 2.14 nm)[11] in In_2O_3, therefore, we exclude the possibility of the observed PL arising from a quantum confinement effect. However, in our case, during the rapid evaporation–oxidation synthesis of In_2O_3 nanowires, oxygen vacancies would be formed because of incomplete oxidation. In addition, the In_2O_3 nanowires with high aspect ratio and peculiar morphologies should also favor the existence of oxygen vacancies.[11] The oxygen vacancies represent new energy levels in the band gap. Furthermore, the electron paramagnetic resonance (EPR) results (in Fig. 5, $g = 2.0069$) reveal that there are many singly ionized oxygen vacancies ($V_O^{\bullet}$) in our In_2O_3 nanowires because other oxygen vacancies (V_O or V_O^{++}) are not paramagnetic.[12] The PL emission thus results from the radiative recombination of a photo-generated hole with an electron occupying the oxygen vacancies (V_O^{+})

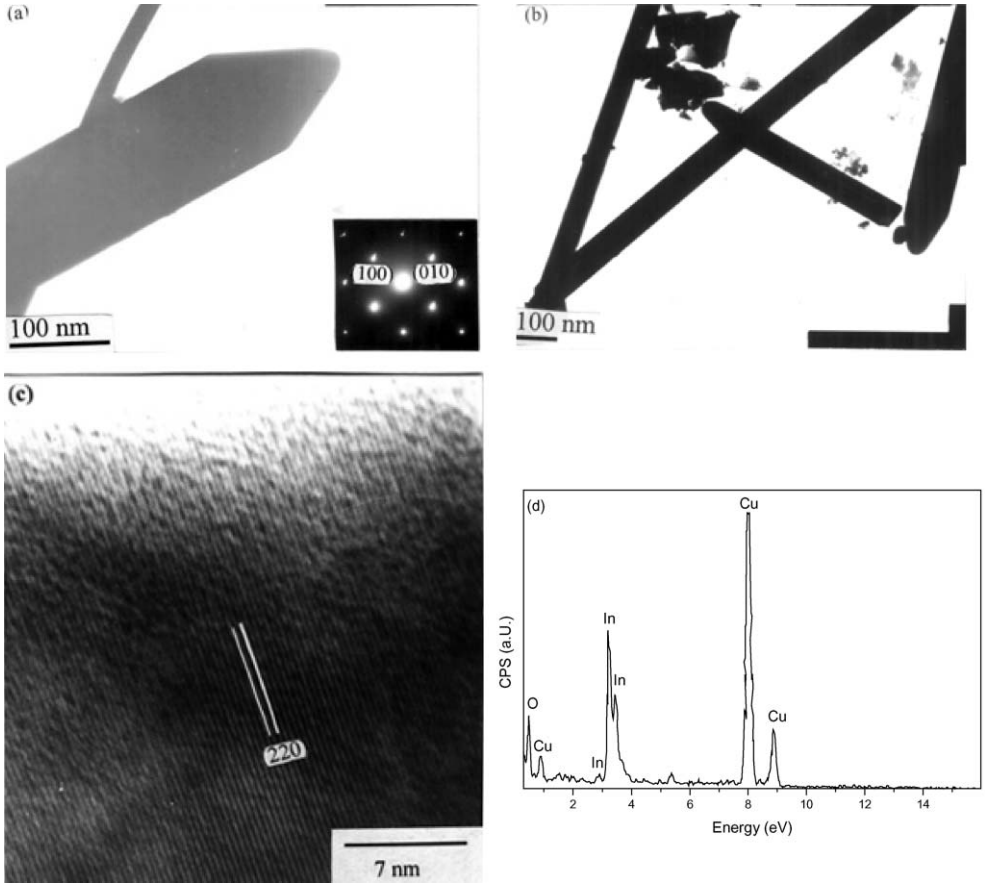

Fig. 3 (a) A typical TEM image of two individual nanowires: one with a cone-tip end and the other thinner wire with diameter of about 40 nm. The insert is the corresponding SAED pattern. (b) TEM image of several In_2O_3 nanowires with conical tip at their end. (c) HRTEM image shows the fine structure of the smaller one shown in Fig. 3(a), the (220) lattice plane is clearly resolved. (d) The corresponding EDX results. The Cu peaks in this spectrum are due to background from the copper TEM grid.

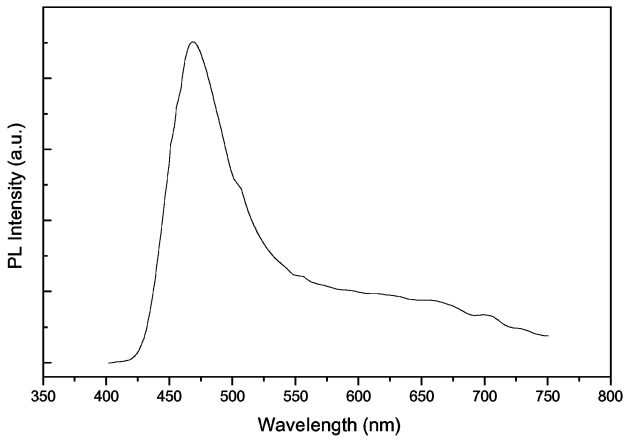

Fig. 4 PL spectrum of the In_2O_3 nanowires at room temperature.

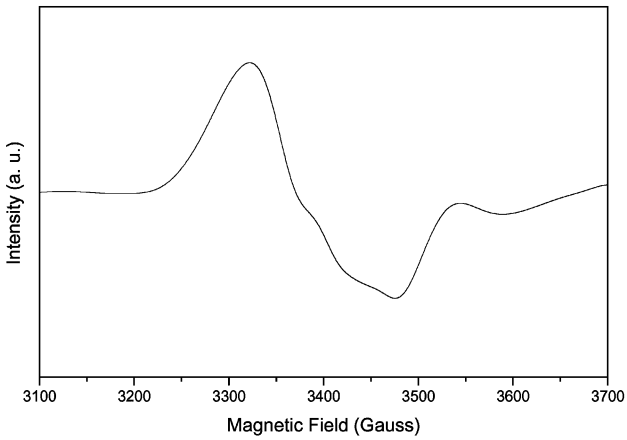

Fig. 5 X-Band (9.45 GHz) EPR traces for the In_2O_3 nanowires at room temperature.

similar to that reported in ref. 12. Therefore we propose that the V_O^+ is most probably responsible for the PL emission in the In_2O_3 nanowires.

Conclusion

In summary, cubic In_2O_3 single-crystalline nanowires were prepared in a high yield *via* a vapor–solid method at 1030 °C. SEM, TEM, XRD and SAED investigations show that the nanowires are quite straight and uniform with diameters of about 40–120 nm, lengths up to 15–25 μm and a cubic In_2O_3 structure. The emission peak at 470 nm from In_2O_3 nanowires was attributed to singly ionized oxygen vacancies V_O^+ confirmed by the EPR results.

Acknowledgements

This work was supported by the Key Project of National Fundamental Research and the Natural Science Foundation of China (Grant No. 19974055).

References

1 J. T. Hu, T. W. Odom and C. M. Lieber, *Acc. Chem. Res.*, 1999, **32**, 435.

2 Z. G. Bai, D. P. Tu, H. Z. Zhang, Y. Ding, X. Z. Gai, Q. L. Hang, G. C. Xiong and S. Q. Feng, *Chem. Phys. Lett.*, 1999, **303**, 311.
3 Y. C. Choi, W. S. Kim, Y. S. Park, S. M. Lee, D. J. Bae, Y. H. Lee, G. S. Park, W. B. Choi, N. S. Lee and J. M. Kim, *Adv. Mater.*, 2000, **12**, 746.
4 P. Yang and C. M. Lieber, *Science*, 1996, **273**, 1836.
5 Y. Q. Zhu, W. B. Hu, W. K. Hsu, M. Terrones, N. Grobert, J. P. Hare, H. W. Kroto, D. R. M. Walton and H. Terrones, *J. Mater. Chem.*, 1999, **9**, 3173.
6 Z. W. Pan, Z. R. Dai and Z. L. Wang, *Science*, 2001, **291**, 1947.
7 C. G. Granqvist, *Appl. Phys. A: Solid Surf.*, 1993, **57**, 19.
8 I. Hamburg and C. G. Granqvist, *J. Appl. Phys.*, 1986, **60**, R123.
9 M. S. Lee, W. C. Choi, E. K. Kim, C. K. Kim and S. K. Min, *Thin Solid Films*, 1996, **279**, 1.
10 H. J. Zhou, W. P. Cai and L. D. Zhang, *Appl. Phys. Lett.*, 1999, **75**, 495.
11 C. H. Liang, G. W. Meng, Y. Lei, F. Phillipp and L. D. Zhang, *Adv. Mater.*, 2001, **13**, 1330.
12 M. J. Zheng, L. D. Zhang, G. H. Li, X. Y. Zhang and X. F. Wang, *Appl. Phys. Lett.*, 2001, **79**, 839.
13 M. Marezio, *Acta Crystallogr.*, 1966, **20**, 273.
14 X. F. Duan and C. M. Lieber, *Adv. Mater.*, 2000, **12**, 298.
15 Z. Cui, G. W. Meng, W. D. Huang, G. Z. Wang and L. D. Zhang, *Mater. Res. Bull.*, 2000, **35**, 10.
16 W. K. Burton, N. Cabrera and F. C. Frank, *Philos. Trans. R. Soc. (London)*, 1951, **243**, 299.
17 W. Van Erk, H. J. G. J. Van Hoek-Martens and G. Bertels., *J. Cryst. Growth*, 1980, **48**, 621.
18 Y. Ohhata and F. Shinoki, *Thin Solid Films*, 1979, **59**, 255.
19 P. Yang and C. M. Lieber, *J. Mater. Res.*, 1997, **12**, 2891.
20 N. M. Lakin, G. van den Hoek, I. R. Beattie and J. M. Brown, *J. Chem. Phys.*, 1997, **107**, 4439.